

Inter-cell Interference Coordination Using Frequency Block Dependent Transmission Power Control and PF Scheduling in Non-orthogonal Access with SIC for Cellular Uplink

Hiromi Katayama[†], Yoshihisa Kishiyama[‡], and Kenichi Higuchi^{†(*)}

[†]Graduate School of Science and Technology, Tokyo University of Science

[‡]Radio Access Network Development Department, NTT DOCOMO, INC.

E-mail: ^(*)higuchik@rs.noda.tus.ac.jp

Abstract—This paper proposes an inter-cell interference coordination (ICIC) method using frequency block-dependent transmission power control (TPC) and proportional fair (PF) scheduling in non-orthogonal access with minimum mean squared error-based linear filtering followed by a successive interference canceller (MMSE-SIC) in the cellular uplink. The proposed method uses TPC coordinated among neighboring cells based on frequency block-dependent parameters. Under this transmission power setting, the use of PF scheduling achieves the ICIC effect. In conventional fractional frequency reuse (FFR) for ICIC in the uplink, users within a cell are categorized into cell-interior and cell-edge user groups and each user group can access only a portion of the frequency blocks. This degrades the multiuser diversity gain and the throughput gain due to non-orthogonal user multiplexing, which is in general increased when the users with largely different channel conditions are multiplexed into the same frequency block. Since all the users within a cell can access all frequency blocks in the proposed method, the method abates the drawbacks of conventional FFR. Simulation results show that non-orthogonal access employing an MMSE-SIC using the proposed ICIC method significantly enhances the system-level throughput performance compared to conventional FFR. We also show the performance gain of non-orthogonal access employing the MMSE-SIC compared to orthogonal access, which is widely used in 3.9 and 4G mobile communication systems.

I. INTRODUCTION

In 3rd generation mobile communication systems such as W-CDMA or cdma2000, non-orthogonal access based on direct sequence-code division multiple access (DS-SS) is widely used. However, the receiver uses simple single-user detection such as a Rake receiver. Orthogonal access based on orthogonal frequency division multiple access (OFDMA) or single carrier-frequency division multiple access (SC-FDMA) is adopted in 3.9 and 4th generation mobile communication systems such as LTE [1] and LTE-Advanced [2].

However, non-orthogonal access can again be a promising candidate as an uplink multiple access scheme for systems beyond those mentioned above. Here, we assume that non-orthogonal access is used with advanced signal detection techniques such as a successive interference canceller (SIC) [3, 4], which is different from the 3rd generation mobile communication systems. Non-orthogonal access with advanced signal detection techniques can improve the system efficiency measured based on the total or average user throughput and

user fairness (cell-edge user experiences). This is because all the users can use the overall transmission bandwidth regardless of the channel conditions in non-orthogonal access, while orthogonal access must restrict the bandwidth assignment to the users under poor channel conditions in order to achieve a sufficiently high average user throughput [5, 6].

In this paper, we investigate an inter-cell interference coordination (ICIC) method appropriate for non-orthogonal access with a SIC in the cellular uplink. The conventional method for ICIC employs frequency reuse between neighboring cells. Fractional frequency reuse (FFR) methods were proposed that allow users under different channel conditions to enjoy different reuse factors [7-9]. The FFR methods basically use a lower reuse factor for cell-edge users because these users are close to a neighboring BS and severe inter-cell interference is expected if the same frequency is reused. Fig. 1 shows a typical FFR method which is referred to as soft FFR herein [9].

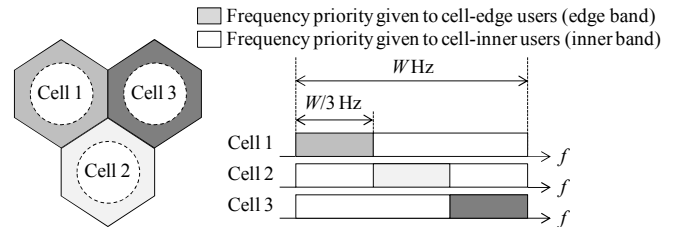


Figure 1. Spectrum usage in soft FFR.

The users within a cell are categorized into cell-interior users and cell-edge users based on the path loss between the user and the serving base station (BS). For the cell-edge user group, 1/3-frequency reuse is used. Thus, 1/3 of the overall transmission bandwidth (hereafter edge band) is dedicated to the cell-edge user group. Among the three neighboring cells as indicated in Fig. 1, the edge bands do not overlap. The cell-interior user group can use the remaining 2/3 of the overall transmission bandwidth (hereafter inner band). Such spectrum usage achieves an ICIC effect [10]. However, the predetermined user categorization into cell-interior and cell-edge user groups and the restriction in frequency assignment to the respective user groups severely degrade the multiuser diversity gain, which largely offsets the ICIC effect. Furthermore, although the non-orthogonal user multiplexing gain compared to orthogonal user

multiplexing is increased when users experiencing good channel conditions are multiplexed with those experiencing bad channel conditions in the same frequency block, the conventional FFR restricts such user multiplexing due to the predetermined user categorization.

To mitigate the above problems in conventional FFR, the proposed method allows all users within a cell to access all the frequency blocks. In order to achieve the ICIC effect, the proposed method uses transmission power control (TPC) that is coordinated among neighboring cells and based on frequency block-dependent parameters. More specifically, assuming the same definition of the edge and inner bands as in conventional FFR, the TPC at the edge band is set so that the cell-edge user can transmit a signal with high power at the edge band. The TPC at the inner band restricts the transmission power of the cell-edge users. Under this transmission power setting, the use of proportional fair (PF) scheduling [11, 12] achieves the ICIC effect. This is because first the PF criteria tends to allocate the edge band to cell-edge users more frequently compared to the inner band (opposite occurs to the cell-interior users). Second, even when the inner band is allocated to a cell-edge user by the scheduler, severe inter-cell interference is avoided since the transmission power of the cell-edge user in the inner band is restricted by the frequency block-dependent TPC.

The remainder of the paper is organized as follows. First, Section II describes the basic system model with non-orthogonal access employing a SIC in the uplink. Section III explains the proposed ICIC method. Then, Section IV presents simulation results on the system-level throughput. Finally, Section V concludes the paper.

II. SYSTEM MODEL

We assume orthogonal frequency division multiplexing (OFDM) signaling using a cyclic prefix (CP) for all users, although we consider non-orthogonal user multiplexing. Therefore, the inter-symbol interference and inter-carrier interference are perfectly eliminated assuming that the length of the CP is sufficiently long so that it covers the entire multipath delay spread. In the paper, the number of transmitter antennas of the user terminal is assumed to be one. The number of receiver antennas at the BS is $N_r = 2$. The number of users per cell is K . There are B frequency blocks and the bandwidth of the frequency block is W . In the following, we consider the signal transmission procedure at a specific n -th BS. The i -th ($1 \leq i \leq K$) user served by BS n is denoted as user (n, i) .

We assume that the multiuser scheduler of BS n schedules a set of users, $S_{n,b} = \{(n, i_b(1)), (n, i_b(2)), \dots, (n, i_b(m_{n,b}))\}$, to frequency block b ($1 \leq b \leq B$), where $(n, i_b(l))$ indicates the l -th ($1 \leq l \leq m_{n,b}$) user index scheduled at frequency block b and $m_{n,b}$ denotes the number of scheduled users at frequency block b of BS n . Here, we assume that the user within $S_{n,b}$ is sorted in the order of the decreasing average user throughput to improve user fairness [6]. In this section, time index t is omitted for simplicity. For user $(n, i_b(l))$, coded modulation symbol $x_b(n, i_b(l))$ ($\mathbb{E}[|x_b(n, i_b(l))|^2] = 1$) is transmitted on a certain subcarrier of frequency block b . The N_r -dimensional

received signal vector, $\mathbf{y}_{n,b}$, at BS n on a certain subcarrier of frequency block b is represented as

$$\mathbf{y}_{n,b} = \sum_{k=1}^{m_{n,b}} \mathbf{h}_b(n, i_b(k)) \sqrt{p_b(n, i_b(k))} x_b(n, i_b(k)) + \mathbf{w}_{n,b}, \quad (1)$$

where $\mathbf{h}_b(n, i_b(k))$ is the N_r -dimensional channel coefficient vector between user $(n, i_b(k))$ and serving BS n at frequency block b , which includes distance-dependent loss, shadowing loss, and instantaneous fading coefficients. For simplicity, we assume here that the instantaneous fading coefficients are kept constant within a frequency block. Term $p_b(n, i_b(k))$ is the transmission power per subcarrier of user $(n, i_b(k))$ at frequency block b . The N_r -dimensional vector, $\mathbf{w}_{n,b}$, is the receiver noise and inter-cell interference vector. We assume that $\mathbf{w}_{n,b}$ consists of i.i.d. circularly complex Gaussian random variables with zero mean and variance $N_{0,n,b}$.

We employ the minimum mean squared error-based linear filtering followed by the successive interference canceller (MMSE-SIC) at the BS receiver. In the MMSE-SIC, the input of the MMSE filtering for signal detection of user $(n, i_b(l))$ is the received signal vector after subtraction of the signal component from user $(n, i_b(1))$ through $(n, i_b(l-1))$, which is a SIC process. Thus, the input of the MMSE filtering for signal detection of user $(n, i_b(l))$ is represented as

$$\mathbf{h}_b(n, i_b(l)) \sqrt{p_b(n, i_b(l))} x_b(n, i_b(l)) + \sum_{k=l+1}^{m_{n,b}} \mathbf{h}_b(n, i_b(k)) \sqrt{p_b(n, i_b(k))} x_b(n, i_b(k)) + \mathbf{w}_{n,b}. \quad (2)$$

The MMSE filter vector for user $(n, i_b(l))$, $\mathbf{c}_b(n, i_b(l))$, is represented as

$$\mathbf{c}_b(n, i_b(l)) = \left(\sum_{k=l}^{m_{n,b}} p_b(n, i_b(k)) \mathbf{h}_b(n, i_b(k)) \mathbf{h}_b^H(n, i_b(k)) + N_{0,n,b} \mathbf{I} \right)^{-1} \cdot \sqrt{p_b(n, i_b(l))} \mathbf{h}_b(n, i_b(l)). \quad (3)$$

The signal-to-interference and noise power ratio (SINR) of $x_b(n, i_b(l))$ at the MMSE-filter output, $\text{SINR}_b(n, i_b(l))$, is represented as

$$\text{SINR}_b(n, i_b(l)) = \frac{\sqrt{p_b(n, i_b(l))} \mathbf{c}_b^H(n, i_b(l)) \mathbf{h}_b(n, i_b(l))}{1 - \sqrt{p_b(n, i_b(l))} \mathbf{c}_b^H(n, i_b(l)) \mathbf{h}_b(n, i_b(l))}. \quad (4)$$

Here, \mathbf{A}^H represents the Hermitian transpose of \mathbf{A} . Therefore, the throughput of user $(n, i_b(l))$ at frequency block b assuming the scheduled user set of $S_{n,b}$, $r_b(n, i_b(l) | S_{n,b})$, is represented as [6]

$$\begin{aligned} r_b(n, i_b(l) | S_{n,b}) &= W \log(1 + \text{SINR}_b(n, i_b(l))) \\ &= W \log \det \left(\mathbf{I} + \frac{\sum_{k=l}^{m_{n,b}} p_b(n, i_b(k)) \mathbf{h}_b(n, i_b(k)) \mathbf{h}_b^H(n, i_b(k))}{N_{0,n,b}} \right) \\ &\quad - W \log \det \left(\mathbf{I} + \frac{\sum_{k=l+1}^{m_{n,b}} p_b(n, i_b(k)) \mathbf{h}_b(n, i_b(k)) \mathbf{h}_b^H(n, i_b(k))}{N_{0,n,b}} \right) \end{aligned} \quad (5)$$

III. PROPOSED ICIC METHOD

In the explanation hereafter, the set of all frequency blocks is denoted as $X = \{1, 2, \dots, B\}$. The proposed method defines the edge and inner bands the same as in the conventional FFR.

At BS n , the sets of frequency blocks belonging to the edge and inner bands are denoted as $X_{\text{edge}}(n)$ and $X_{\text{inner}}(n)$, respectively. Here, $|X_{\text{edge}}(n) \cap X_{\text{inner}}(n)| = 0$ and $X_{\text{edge}}(n) \cup X_{\text{inner}}(n) = X$. Between neighboring BS n and BS n' , $|X_{\text{edge}}(n) \cap X_{\text{edge}}(n')| = 0$.

Basically, we use the fractional TPC method in the paper, which is applied in LTE [13, 14]. Although fractional TPC in LTE assumes the same parameters for all frequency blocks, the proposed method uses a frequency block-dependent parameter setting. In the proposed frequency block-dependent fractional TPC, the transmission power per subcarrier in decibels (referenced in milliwatts) (dBm) of the k -th user at BS n (user (n, k)) at frequency block b , $p_b^{(\text{FTPC})}(n, k)$, is determined as

$$p_b^{(\text{FTPC})}(n, k) = \min(T_0(n, b) + P_{\text{noise}} + \alpha(n, b)L(n, k), P_{\text{max}}), \quad (6)$$

where $T_0(n, b)$ is the target signal-to-noise ratio (SNR) in decibel notation at frequency block b of BS n , and P_{noise} is the receiver noise power per frequency block both in dBm. Term P_{max} is the maximum transmission power. Term $L(n, k)$ is the average path loss (distance-dependent loss and shadowing loss) between user (n, k) and serving BS n in decibel notation. Parameter $\alpha(n, b)$ ($0 < \alpha(n, b) \leq 1$) is the compensation factor of the average path loss at frequency block b of BS n . When $\alpha(n, b)$ is one, the received average SNR for all users is maintained at $T_0(n, b)$. However, in this case, the transmission power of the cell-edge user may be significantly high, which results in severe inter-cell interference. The use of an $\alpha(n, b)$ value lower than one, which partially compensates for the average path loss, achieves a tradeoff between the inter-cell interference level and the signal reception quality of the cell-edge users.

In order to obtain the ICIC effect, coordination of $T_0(n, b)$ and $\alpha(n, b)$ among cells is essential. In the paper, we define $T_0(n, b)$ and $\alpha(n, b)$ respectively as

$$T_0(n, b) = \begin{cases} T_{0, \text{edge}}, & b \in X_{\text{edge}}(n) \\ T_{0, \text{inner}}, & b \in X_{\text{inner}}(n) \end{cases}, \quad (7)$$

$$\alpha(n, b) = \begin{cases} \alpha_{\text{edge}}, & b \in X_{\text{edge}}(n) \\ \alpha_{\text{inner}}, & b \in X_{\text{inner}}(n) \end{cases}. \quad (8)$$

Thus, $T_0(n, b)$ and $\alpha(n, b)$ in the edge and inner bands are separately defined. The purpose of frequency block-dependent TPC is to reduce the inter-cell interference caused at the inner band compared to that caused at the edge band for ICIC. In general, the use of a higher α value increases the transmission power of the cell-edge users relative to the cell-interior users, which results in an increase in inter-cell interference. Therefore, we set $\alpha_{\text{edge}} > \alpha_{\text{inner}}$ in the proposed method. Furthermore, as T_0 increases, P_{max} tends to limit the transmission power of the cell-edge users. Therefore, we set $T_{0, \text{edge}} < T_{0, \text{inner}}$ in the proposed method. With this parameter setting, the transmission power of the cell-edge user at the inner band is restricted more than that at the edge band, and the received signal power gap between the cell-edge user and cell-interior user becomes wider at the inner band.

In non-orthogonal access, the number of transmitting users within a frequency block is $|S_{n,b}| \geq 1$. Therefore, compared to orthogonal access in which $|S_{n,b}|$ is always one, inter-cell

interference may be increased due to the increased total transmission signal energy per cell. The increased inter-cell interference will offset the gain by using non-orthogonal access with the MMSE-SIC. To address this problem, we use the following TPC [6] to modify $p_b^{(\text{FTPC})}(n, k)$ according to the candidate set of scheduled users, S . For a given S , the final transmission power in Watts per subcarrier, $p_b(n, k | S)$, $k \in S$, is determined as

$$p_b(n, k | S) = \min \left(\left(\frac{\max_{l \in S} p_b^{(\text{FTPC})}(n, l)}{\sum_{l \in S} p_b^{(\text{FTPC})}(n, l)} \right) p_b^{(\text{FTPC})}(n, k), p_b^{(\text{FTPC})}(n, k) \right). \quad (9)$$

Thus, the total transmission power at frequency block b is restricted to the maximum basic transmission power per user, which is determined using the proposed fractional TPC, among users belonging to candidate scheduled user set S .

After the above TPC process, the multiuser scheduler allocates a frequency block to more than one user simultaneously. We use the PF scheduler [11, 12], which is known to achieve a good tradeoff between the system efficiency and user fairness by maximizing the product of the average user throughput among users within a cell. In [12], the multiuser scheduling version of the PF scheduler is presented.

The average user throughput of user (n, k) per frequency block is defined as

$$\bar{r}(n, k; t) = \left(1 - \frac{1}{t_c} \right) \bar{r}(n, k; t-1) + \frac{1}{t_c} \left(\frac{1}{B} \sum_{b=1}^B r_b(n, k; t-1) \right), \quad (10)$$

where t denotes the discrete time index representing a subframe index. Parameter t_c defines the time horizon for throughput averaging. We assume t_c of 100 with the subframe length of 1 ms in the following evaluation. Term $r_b(n, k; t-1)$ is the throughput of user (n, k) in frequency block b at time instance $t-1$. Throughput $r_b(n, k; t-1)$ is calculated using (5) for given $\{p_b(n, k | S_{n,b})\}$ at time $t-1$ and is zero if user (n, k) is not scheduled at frequency block b at time $t-1$.

Under proportional fairness, the multiuser scheduling policy that maximizes the product of the average user throughput among users within a cell selects user set $S_{n,b}$ according to the following criteria [12].

$$f_{n,b}(S; t) = \prod_{k \in S} \left(1 + \frac{r_b(n, k | S; t)}{(t_c - 1) \bar{r}(n, k; t)} \right). \quad (11)$$

$$S_{n,b}(t) = \arg \max_S f_{n,b}(S; t). \quad (12)$$

Term $f_{n,b}(S; t)$ is the scheduling metric for user set S , and user set S that maximizes the scheduling metric is selected as $S_{n,b}$ at time t .

In the proposed method, since the user is located near the cell edge, $r_b(n, k | S_{n,b}; t)$ for $b \in X_{\text{edge}}(n)$ tends to be higher than $r_b(n, k | S_{n,b}; t)$ for $b \in X_{\text{inner}}(n)$ on average due to the proposed frequency block-dependent TPC. Therefore, the scheduler allocates the edge band to the cell-edge user more frequently than the inner band, similar to conventional FFR. However, since all the users are candidates for all frequency blocks in the proposed method, depending on the instantaneous channel

condition, the cell-edge and cell-interior users can also use the inner and edge bands, respectively. This increases the multiuser diversity via the channel-aware PF scheduler and allows for non-orthogonal multiplexing of users under largely different channel conditions. Even when the inner band is allocated to the cell-edge user, severe inter-cell interference is avoided since the transmission power of the cell-edge user at the inner band is restricted by the proposed frequency block-dependent TPC.

IV. SIMULATION RESULTS

We evaluated the distribution of the user throughput in a multi-cell uplink. Table I gives the simulation parameters. These parameters basically follow the evaluation assumptions in 3GPP LTE [15]. A 19-cell model with a hexagonal grid assuming universal frequency reuse is used. The inter-site (BS) distance is 500 m. The number of users per cell, K , is set to 30. The locations of the user terminals in each cell are randomly assigned with a uniform distribution. The values of W and B are set to 180 kHz and 24, respectively (overall transmission bandwidth is 4.32 MHz). The maximum transmission power of the user terminal is 24 dBm. In the propagation model, we took into account distance-dependent path loss with the decay factor of 3.76, lognormal shadowing with the standard deviation of 8 dB and 0.5-correlation among sites, 6-path Rayleigh fading with the rms delay spread of 1 μ s, and the maximum Doppler frequency of 55.5 Hz. The receiver noise density of the BS is set to -169 dBm/Hz.

TABLE I. SIMULATION PARAMETERS

| Cell layout | | Hexagonal 19-cell model |
|---|--------------------|---|
| Inter-site distance | | 0.5 km |
| Overall transmission bandwidth | | 4.32 MHz |
| Resource block bandwidth | | 180 kHz |
| Number of resource blocks | | 24 |
| Number of user terminals per cell | | 30 |
| BS receiver antenna | Number of antennas | 2 |
| | Antenna gain | 14 dBi |
| User terminal transmitter antenna | Number of antennas | 1 |
| | Antenna gain | 0 dBi |
| Maximum transmission power of user terminal | | 24 dBm |
| Distance-dependent loss | | $128.1 + 37.6 \log_{10}(r)$ dB, r : kilometers |
| Lognormal shadowing | | Standard deviation = 8 dB Correlation among cells = 0.5 |
| Instantaneous fading | | Six-path Rayleigh, rms delay spread = 1 μ s, $f_D = 55.5$ Hz |
| Receiver noise density | | -169 dBm/Hz |
| Scheduling interval | | 1 ms |
| Throughput calculation | | Based on Shannon formula (Max. 6 b/s/Hz) |
| Averaging interval for user throughput | | 100 ms ($t_c = 100$) |

The radio resource allocation is updated in 1-ms intervals. The user throughput averaged over 100 ms is measured according to the assumption in [15]. The user throughput is calculated based on the Shannon formula with the maximum of 6 b/s/Hz (corresponding to 64QAM). The maximum number of non-orthogonally multiplexed users per frequency block, N_{\max} , is set to four. In the scheduling, all possible user sets S with $|S| \leq 4$ are examined and the user set achieving the highest scheduling metric is selected. In the following, we evaluate the average user throughput within a cell, R_{avg} . We also evaluate

the cell-edge user throughput, R_{edge} , which is defined as the user throughput value at the cumulative probability of 5% according to the assumption in LTE [15].

Fig. 2 shows R_{edge} and R_{avg} as a function of $T_{0,\text{inner}}$ where $\{T_{0,\text{edge}}, \alpha_{\text{inner}}, \alpha_{\text{edge}}\}$ are set to $\{55 \text{ dB}, 0.5, 0.8\}$. As $T_{0,\text{inner}}$ is increased from 40 dB, R_{edge} and R_{avg} are increased due to the increased SNR. However, when $T_{0,\text{inner}}$ is increased beyond approximately 70 dB, R_{edge} decreases, although R_{avg} further increases. This is because the transmission power of the cell-edge users is limited by P_{\max} when $T_{0,\text{inner}}$ is excessively high.

Fig. 3 shows R_{edge} and R_{avg} as a function of $T_{0,\text{edge}}$ where $\{T_{0,\text{inner}}, \alpha_{\text{inner}}, \alpha_{\text{edge}}\}$ are set to $\{75 \text{ dB}, 0.5, 0.8\}$. As $T_{0,\text{edge}}$ is increased from 40 dB, R_{edge} and R_{avg} initially increase. However, if $T_{0,\text{edge}}$ increases beyond 50 dB, R_{avg} decreases. This is mainly due to the increased inter-cell interference caused at the edge band. When $T_{0,\text{edge}}$ increases beyond 60 dB, R_{edge} also decreases since the transmission power of the cell-edge users is limited by P_{\max} at the edge band. Therefore, the inner band is allocated to the cell-edge users more frequently, which reduces the ICIC effect. From Figs. 2 and 3, we confirm the effectiveness of the setting $T_{0,\text{edge}} < T_{0,\text{inner}}$ in the proposed method.

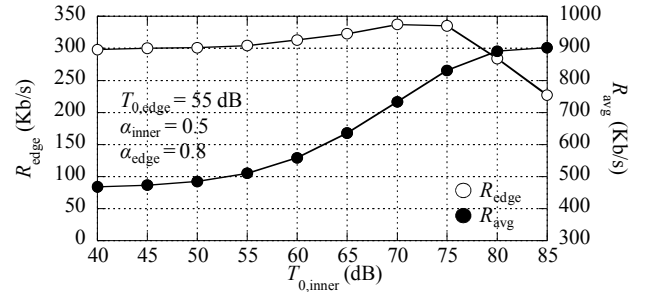


Figure 2. R_{edge} and R_{avg} as a function of $T_{0,\text{inner}}$.

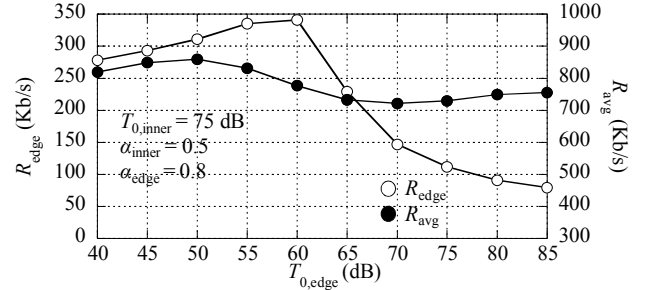


Figure 3. R_{edge} and R_{avg} as a function of $T_{0,\text{edge}}$.

Fig. 4 shows R_{edge} and R_{avg} as a function of α_{inner} where $\{T_{0,\text{inner}}, T_{0,\text{edge}}, \alpha_{\text{edge}}\}$ are set to $\{75 \text{ dB}, 55 \text{ dB}, 0.8\}$. Higher α_{inner} values degrade R_{edge} since the transmission power of the cell-edge users tends to be limited by P_{\max} at the inner band and the ICIC effect is reduced. Fig. 5 shows R_{edge} and R_{avg} as a function of α_{edge} where $\{T_{0,\text{inner}}, T_{0,\text{edge}}, \alpha_{\text{inner}}\}$ are set to $\{75 \text{ dB}, 55 \text{ dB}, 0.5\}$. As α_{edge} is increased from 0.5, R_{edge} and R_{avg} initially increase since the transmission power of the cell-edge users is increased at the edge band. This results in more frequent edge band assignment to the cell-edge users, which enhances the ICIC effect. However, an excessively high α_{edge} value decreases both R_{edge} and R_{avg} . Figs. 4 and 5 confirm the effectiveness of setting $\alpha_{\text{edge}} > \alpha_{\text{inner}}$ in the proposed method.

Fig. 6 compares R_{edge} and R_{avg} of the proposed method to that with universal frequency reuse (UFR) and conventional FFR. For the proposed method, $\{T_{0,\text{inner}}, T_{0,\text{edge}}, \alpha_{\text{inner}}, \alpha_{\text{edge}}\}$ are set to $\{75 \text{ dB}, 55 \text{ dB}, 0.5, 0.8\}$. In FFR, 10 users among 30 users within a cell are categorized into the cell-edge user group. For UFR and FFR, $\{T_{0,\text{inner}} = T_{0,\text{edge}}, \alpha_{\text{inner}} = \alpha_{\text{edge}}\}$ are set to $\{56 \text{ dB}, 0.6\}$ and $\{70 \text{ dB}, 0.5\}$, respectively, so that R_{avg} of UFR and FFR becomes approximately the same as that for the proposed method. For comparison, UFR with N_{max} of 1, which corresponds to orthogonal access (OFDMA), is also tested with $\{T_{0,\text{inner}} = T_{0,\text{edge}}, \alpha_{\text{inner}} = \alpha_{\text{edge}}\}$ of $\{56 \text{ dB}, 0.6\}$. R_{edge} of FFR is rather degraded compared to UFR due to the decreased multiuser diversity and non-orthogonal user multiplexing gain. The proposed method increases R_{edge} by approximately 20% compared to the UFR while almost the same R_{avg} is achieved. We can also see that non-orthogonal access with an MMSE-SIC can significantly enhance R_{avg} and R_{edge} simultaneously compared to orthogonal access.

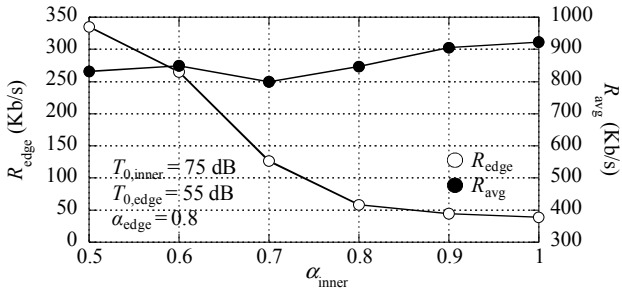


Figure 4. R_{edge} and R_{avg} as a function of α_{inner} .

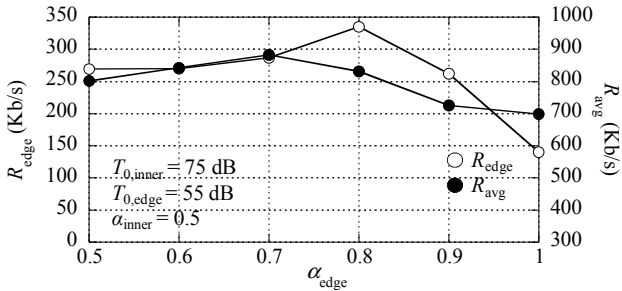


Figure 5. R_{edge} and R_{avg} as a function of α_{edge} .

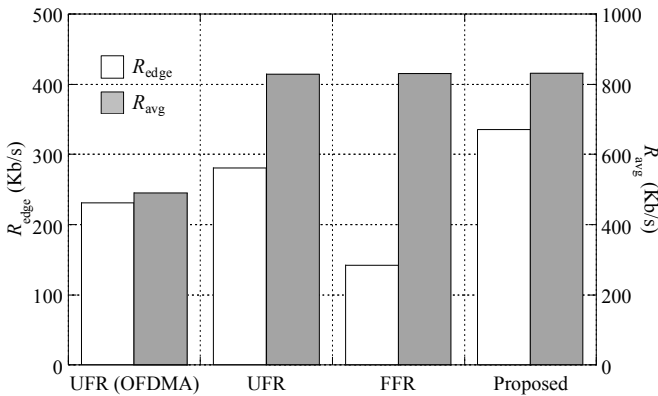


Figure 6. Comparison of R_{edge} and R_{avg} .

V. CONCLUSION

This paper proposed an ICIC method using frequency block-dependent TPC and PF scheduling in non-orthogonal access with an MMSE-SIC in the cellular uplink. In order to mitigate the problem in conventional FFR, which includes degradations in the multiuser diversity gain with PF scheduling and the non-orthogonal user multiplexing gain, the proposed method performs PF scheduling subject to the frequency block-dependent TPC, which is coordinated among neighboring cells. Since all users are candidates for all frequency blocks in the proposed method, depending on the instantaneous channel condition, the cell-edge and cell-interior users can use the inner and edge bands. This increases the multiuser diversity via the channel-aware PF scheduler and allows for non-orthogonal multiplexing of users under largely different channel conditions. Even when the inner band is allocated to the cell-edge user, severe inter-cell interference is avoided since the transmission power of the cell-edge user in the inner band is restricted by the frequency block-dependent TPC. Simulation results showed that non-orthogonal access employing an MMSE-SIC using the proposed ICIC method significantly enhances the system-level throughput performance compared to conventional UFR and FFR. The performance gain of non-orthogonal access with an MMSE-SIC compared to orthogonal access was also shown.

REFERENCES

- [1] 3GPP TS36.300, Evolved Universal Terrestrial Radio Access (E-UTRA) and Evolved Universal Terrestrial Radio Access Network (E-UTRAN); Overall description.
- [2] 3GPP TR36.814 (V9.0.0), "Further advancements for E-UTRA physical layer aspects," Mar. 2010.
- [3] A. D. Wyner, "Shannon-theoretic approach to a Gaussian cellular multiple-access channel," IEEE Trans. Inf. Theory, vol. 40, no. 6, pp. 1713–1727, Nov. 1994.
- [4] O. Somekh and S. Shamai, "Shannon-theoretic approach to a Gaussian cellular multiple-access channel with fading," IEEE Trans. Inf. Theory, vol. 46, no. 4, pp. 1401–1425, July 2000.
- [5] T. Takeda and K. Higuchi, "Enhanced user fairness using non-orthogonal access with SIC in cellular uplink," in Proc. IEEE VTC2011-Fall, San Francisco, U.S.A., 5–8 Sept. 2011.
- [6] Y. Endo, Y. Kishiyama, and K. Higuchi, "Uplink non-orthogonal access with MMSE-SIC in the presence of inter-cell interference," in Proc. IEEE ISWCS 2012, Paris, France, 28–31 Aug. 2012.
- [7] S. E. Elayoubi, O. B. Haddada, and B. Fouresterie, "Performance evaluation of frequency planning schemes in OFDMA-based networks," IEEE Trans. Wireless Commun., vol. 7, no. 5, pp. 1623–1633, May 2008.
- [8] R. Giuliano, C. Monti, and P. Loreti, "WiMAX fractional frequency reuse for rural environments," IEEE Wireless Commun. Mag., vol. 15, no. 3, pp. 60–65, June 2008.
- [9] X. Mao, A. Maaref, and K. H. Teo, "Adaptive soft frequency reuse for inter-cell interference coordination in SC-FDMA based 3GPP LTE uplinks," in Proc. IEEE Globecom2008, New Orleans, U.S.A., Nov. 2008.
- [10] G. Boudreau, J. Panicker, N. Guo, R. Chang, N. Wang, and S. Vrzic, "Interference coordination and cancellation for 4G networks," IEEE Commun. Mag., vol. 47, no. 4, pp. 74–81, Apr. 2009.
- [11] A. Jalali, R. Padovani, and R. Pankaj, "Data throughput of CDMA-HDR a high efficiency-high data rate personal communication wireless system," in Proc. IEEE VTC2000-Spring, May 2000.
- [12] M. Kountouris and D. Gesbert, "Memory-based opportunistic multi-user beamforming," in Proc. IEEE Int. Symp. Information Theory (ISIT), Adelaide, Australia, Sept. 2005.
- [13] W. Xiao, R. Ratasuk, A. Ghosh, R. Love, Y. Sun, and R. Nory, "Uplink power control, interference coordination and resource allocation for 3GPP E-UTRA," in Proc. IEEE VTC2006-Fall, Montréal, Canada, Sep. 2006.
- [14] 3GPP, TS 36.213, "Evolved Universal Terrestrial Radio Access (E-UTRA); Physical layer procedures," May 2009.
- [15] 3GPP, TR 25.814 (V7.0.0), "Physical layer aspects for Evolved UTRA," June 2006.